xCELLigence® RTCA Handbook

Infectious Disease Applications

ACEA Biosciences, Inc.

Infectious Disease Assays in Real-Time

The *in vitro* monitoring of host-pathogen interactions has a long history of being used for both clinical diagnosis and mechanistic studies. In both of these contexts, host-pathogen interactions can be analyzed at either the cellular or molecular levels. At the cellular level, pathogen-induced changes in the host cell can be monitored via different types of microscopy or colorimetric assays. A prime example of this is the cytopathic effect induced by viruses, where infected host cells display rounding/swelling, detachment from the substrate, lysis, etc. The formation of inclusion bodies that are visible by microscopy, as occurs during the intracellular infection of fibroblasts by the *Chlamydia* bacterium, is another example. Alternatively, the live/dead status of pathogen-infected cells can be assessed via colorimetric assays using reagents such as MTT.

At the molecular level, host-pathogen interactions can be studied by monitoring diverse phenomena such as suppression of host DNA or mRNA synthesis, the rerouting of host proteins to different intracellular compartments, modification of chromatin structure, or altered phosphorylation patterns. The myriad techniques used for these molecular analyses include everything from qPCR and flow cytometry to DNA sequencing and Western blotting.

A major shortcoming for the vast majority of the traditional cellular and molecular assays used for identifying, quantifying, and tracking infectious diseases in the clinic or research lab is that they are endpoint assays, providing a mere snapshot of the infection process. As such, kinetic information is difficult or impossible to derive, and one must often extrapolate or interpolate using a limited number of data points. Moreover, many of the traditional assays require labeling which can reduce the assay's physiological relevance, and are low throughput and laborious, requiring multiple sample handling steps that introduce variability. Accordingly, *in vitro* infectious disease studies would greatly benefit from a label-free assay that couples information-rich real-time kinetics with an easy workflow, high reproducibility, and high throughput capabilities. This handbook describes how the xCELLigence Real-Time Cell Analysis® (RTCA) instruments deliver each of these attributes in the context of live cell assays. Example data from diverse bacterial, viral, and parasite applications are used to highlight the extreme utility of RTCA for infectious disease applications.

Table of Contents

xCELLigence RTCA Instruments

The seven different xCELLigence RTCA instruments made by ACEA Biosciences all use noninvasive electrical impedance monitoring (which is explained in the next section) to quantify cell proliferation, morphology change, cell-cell adhesion (i.e. barrier function), and cell-substrate attachment quality in a label-free and real-time manner. The four xCELLigence instruments that are best suited for infectious disease studies are shown in the table below. Besides differing in their plate format/throughput, some of the instruments possess specialized functionalities, such as the ability to monitor cell invasion/migration.

	DP (Dual Purpose)	SP (Single Plate)	MP (Multi Plate)	HT (High Throughput)
Format	3x16 wells	1x96 wells	6x96 wells	1x384 wells
Maximum Throughput	48 wells	96 wells	576 wells	Up to 4x382 wells (1536 wells total)

The xCELLigence RTCA instruments are typically housed inside a standard CO_2 cell culture incubator or hypoxia chamber and are controlled by a laptop computer which sits outside the incubator **(Figure 1)**. Intuitive software enables real-time interfacing with the instrument, and includes real-time data display and analysis functions.

Figure 1. Example of an xCELLigence instrument. The instrument is placed inside a standard tissue culture incubator and is compatible with the full range of biologically relevant temperatures, atmospheric compositions, and humidities. The instrument is controlled by a laptop computer that is housed outside the incubator.

Cellular Impedance

The functional unit of the cellular impedance assay that is run by xCELLigence instruments is a set of gold microelectrodes embedded in the bottom surface of a microtiter plate well **(Figure 2)**. When submersed in an electrically conductive solution (such as buffer or standard tissue culture medium), the application of a weak electric potential across these electrodes causes current to flow between them. Because this phenomenon is dependent upon the electrodes interacting with bulk solution, the presence of adherent cells at the electrode-solution interface impedes current flow. The magnitude of this impedance is dependent upon the number of cells, the size of the cells, cell-cell adhesion (i.e. barrier function), and the cell-substrate attachment quality. Importantly, neither the gold microelectrode surfaces nor the applied electric potential have an effect on cell health or behavior.

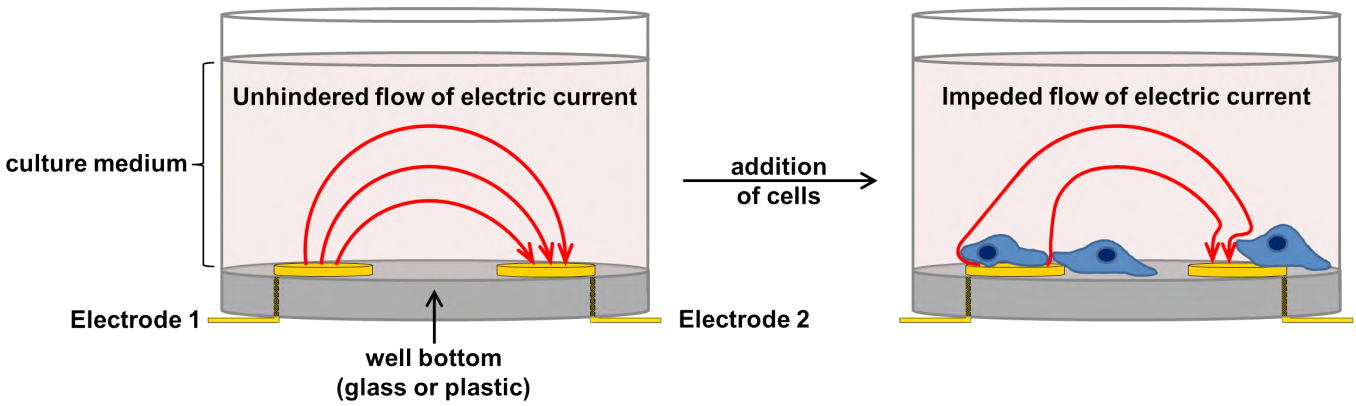

Figure 2. Overview of cellular impedance apparatus. A side view of a single well is shown before and after cells have been added. Neither the electrodes nor the cells are drawn to scale (they have been enlarged for clarity). In the absence of cells electric current flows freely through culture medium, completing the circuit between the electrodes. As cells adhere to and proliferate on the electrodes current flow is impeded, providing an extremely sensitive readout of multiple parameters.

E-Plates®

The gold microelectrode biosensors in each well of ACEA's electronic microtiter plates (E-Plates®) cover ~75% of the bottom's surface area. Rather than the simplified electrode pair depicted in Figure 2, the circular electrodes in each well of an E-Plate are linked into "strands" that form an interdigitating array **(Figure 3)**. This proprietary design enables large populations of cells to be monitored simultaneously and thereby provides exquisite sensitivity to changes in cell number, size, and attachment strength.

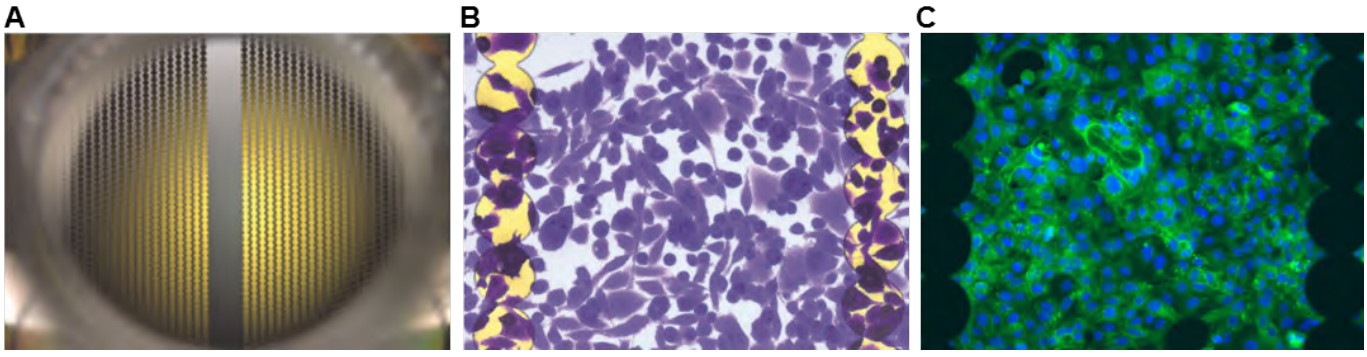

Figure 3. Impedance electrodes in ACEA's E-Plates. (A) Photograph of a single well in an E-Plate. Though cells can also be visualized on the gold electrode surfaces, the electrode-free region in the middle of the well facilitates microscopic imaging. **(B)** Gold electrodes and crystal violet stained human cells, as viewed in a reflected light microscope. **(C)** Immunofluorescence microscopy with gold electrodes silhouetted.

Real-Time Impedance Traces Explained

The impedance of electric current that is caused by adherent cells is reported using a unitless parameter called Cell Index (CI), where CI = (impedance at time point n - impedance in the absence of cells)/(nominal impedance constant). **Figure 4** provides a generic example of a real-time impedance trace throughout the course of setting up and running an apoptosis experiment. For the first few hours after cells have been added to a well there is a rapid increase in impedance, which is caused by cell attachment and spreading. If cells are sub-confluent after the initial attachment stage, they will start to proliferate, causing a gradual yet steady increase in CI. When cells reach confluence the CI value plateaus, reflecting the fact that the electrode surface area that is accessible to bulk media is no longer changing. The addition of an apoptosis inducer, such as a bacterial toxin, at this point causes a decrease in CI back down to zero. This is the result of cells rounding and then detaching from the well bottom. While this generic example involves addition of the apoptosis inducer at the point of cellular confluence, impedance-based assays are extremely flexible and can interrogate a wide variety of phenomena across the full spectrum of cell densities.

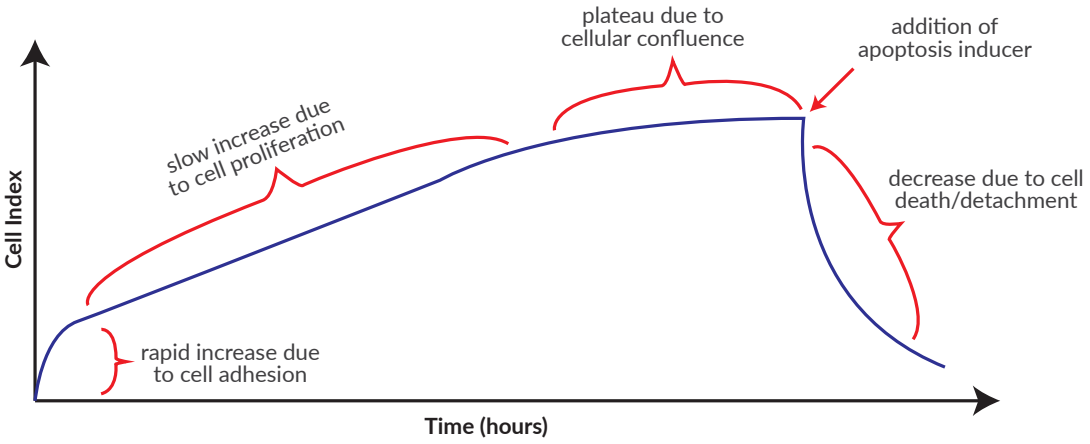

Figure 4. Generic real-time impedance trace for setting up and running an apoptosis assay. Each phase of the impedance trace, and the cellular behavior it arises from, is explained in the text.

Broad Adoption of xCELLigence RTCA

To date, more than 2,000 xCELLigence instruments have been placed globally in labs that span everything from academia and biotech startups to contract research organizations and big pharma. This has resulted in >1,400 xCELLigence publications in peer-reviewed journals **(Figure 5)**. A large, and growing, percentage of these papers are focused on infectious diseases.

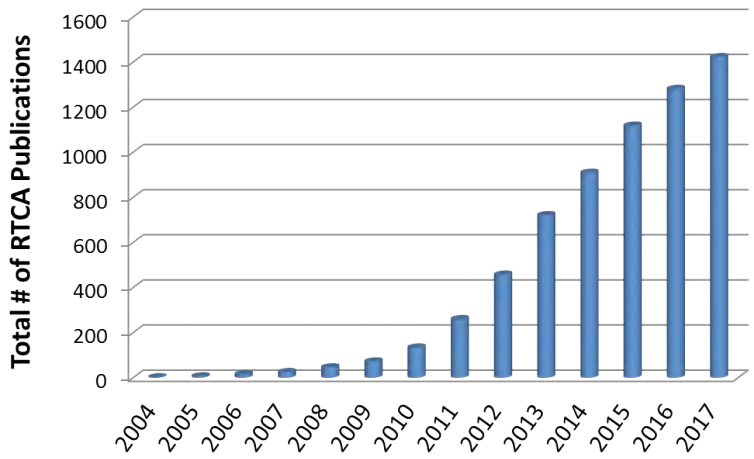

Figure 5. Total number of xCELLigence RTCA publications as a function of time.

RTCA excels at monitoring the dynamic changes in cell number, morphology, and adhesion strength that are induced in host cells as they interact with bacterial toxins, and has been used extensively for this purpose with *Vibrio cholera toxin*[1], *Clostridium botulinum toxin*[2], and *Clostridium difficile toxin*[3-4], as described below.

C. difficile is recognized as a significant nosocomial and community-acquired pathogen in both children and adults, leading to infectious diarrhea that develops in patients after hospitalization and/or receiving antibiotic treatment. Because *C. difficile* protein toxins A and B are the key determinants of virulence, a definitive diagnosis of *C. difficile* infection (CDI) requires detection of either these proteins or the genes that encode them. Historically, the gold standard for *C. difficile* diagnosis has been a cytotoxigenic assay wherein stool samples are incubated *in vitro* and then tested for the presence of protein toxin by monitoring the sample's effect on cultured human cells[5]. Although this cytotoxigenic assay is informative, it is not widely used in clinical settings because it is labor-intensive, subjective, and time-consuming. As alternatives, several enzyme immunoassays (EIAs) and PCR-based toxin gene detection assays approved by the Food and Drug Administration are routinely used in clinical laboratories[6]. However, these suffer from the following drawbacks: EIAs have low sensitivity, and the correlation between toxin gene detection by PCR and disease onset is a matter of debate. Moreover, highly sensitive PCR-based assays can lead to overdiagnosis of CDI and unnecessary therapy because they don't distinguish bona fide *C. difficile* infection from mere colonization[7]. Taken together, CDI diagnosis clearly remains controversial, and a rapid and objective assay with an easy work flow is still needed.

The use of RTCA for quantitative detection of *C. difficile* toxin has been reported by multiple groups[4-6]. In one of these studies HS27 human fibroblast cells were exposed to different concentrations of purified *C. difficile* toxin B[4]. As seen in **Figure 6A**, after allowing the cells to grow to the point of confluence, at which point the impedance signal plateaued, purified toxin was added and its effects were monitored as a time- and dose-dependent decrease in the Cell Index (which correlates with toxin-induced cell death and detachment). This assay was readily able to detect *C. difficile* toxin B at concentrations as low as 0.05 ng/mL, and displayed no cross-reactivity with other enterotoxins, non-toxigenic *C. difficile*, or other *Clostridium* species (data not shown here). In order to develop a standard curve that could be used for determining the concentration of *C. difficile* toxin B in clinical samples, the time required for the normalized Cell Index to drop to 50% of its initial value (i.e. immediately prior to toxin treatment) was then plotted as a function of the toxin concentration to generate the curve shown in **Figure 6B**.

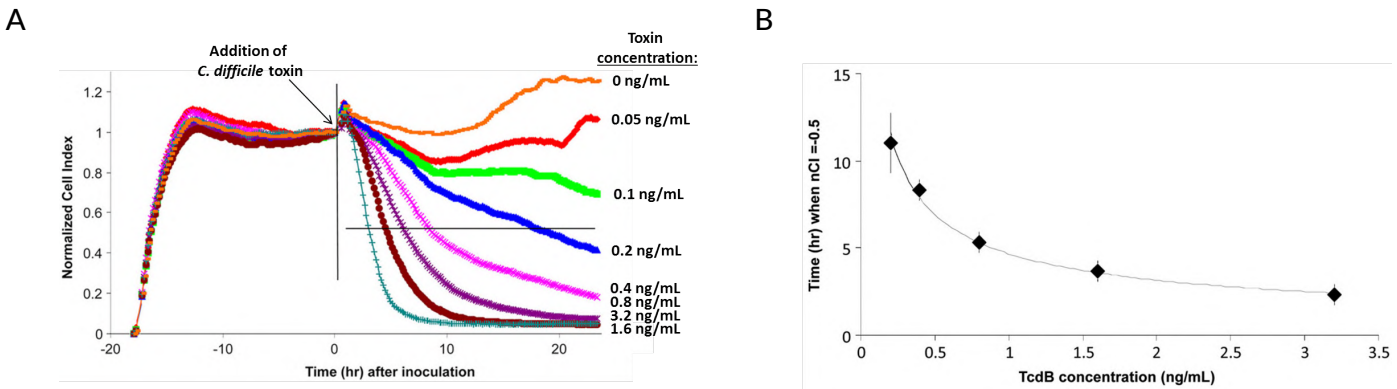

Figure 6. Quantitative detection of *C. difficile* toxin B using xCELLigence RTCA. (A) HS27 cells (5,000 cells/well) were cultivated in E-plate wells, and cell attachment and spreading were monitored in real-time for 17.5 hours before the addition of purified *C. difficile* toxin B at different concentrations. The cytotoxic effect was then monitored continuously for the next ~24 hours. The black vertical line denotes the time of toxin addition (t = 0). The bold horizontal line in the middle of the plot represents a 50% decrease in Cell Index, relative to its starting value (i.e. immediately prior to toxin addition). This is referred to as the normalized Cell Index 50% value, or "nCI=0.5". As expected, the time required for reaching nCI=0.5 is dependent on the concentration of the toxin. **(B)** By plotting nCI=0.5 as a function of toxin concentration, a standard curve was developed, which can be used for determining the concentration of toxin in clinical samples. Data adapted from reference 3.

Clinical validation of the above RTCA *C. difficile* toxin assay was performed using 300 stool specimens from patients with suspected *C. difficile* infection. A sample was scored as being positive or negative for *C. difficile* toxin depending on whether or not it caused a time-dependent drop in normalized Cell Index that could be rescued by the addition of a toxin-specific neutralizing antibody **(Figure 7)**. This RTCA-based scoring approach showed very good correlation with standard cytotoxicity detection using immunohistochemistry/microscopy **(Figure 7)**.

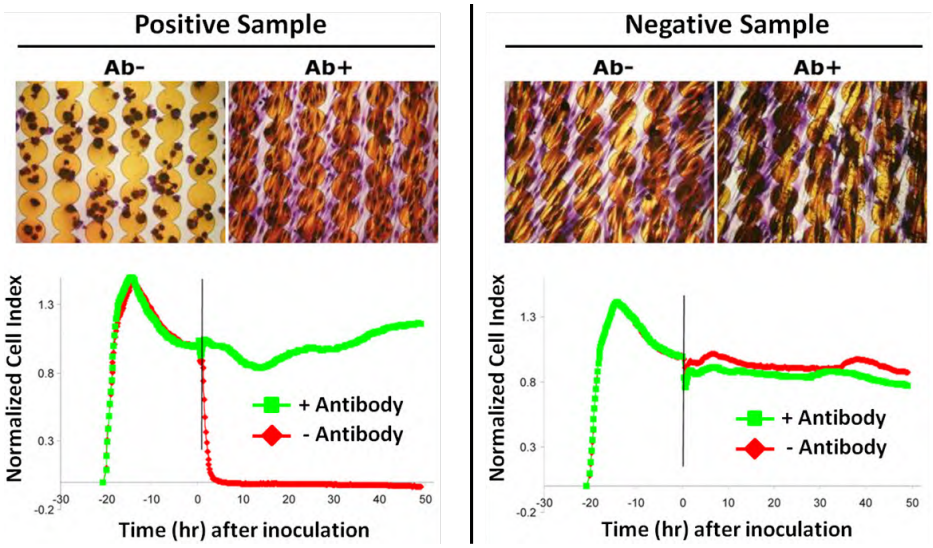

Figure 7. Testing for the presence of *C. difficile* toxin in stool samples from infected and uninfected patients. The RTCA assay described in the text was performed in parallel with a conventional cytotoxicity assay wherein cells were stained and analyzed by microscopy directly in E-Plate wells. The cytotoxic effect is readily visible in the positive sample when using either microscopy or the RTCA assay. As expected, the addition of neutralizing antibody abolishes the cytotoxic effect of *C. difficile* toxin present in the positive sample, but has no impact on the negative sample from an uninfected patient. Data adapted from reference 3.

Using *C. difficile* toxin B as an example, the above study demonstrates that RTCA is an effective tool for applications involving bacterial toxins. Through the use of a standard curve and a neutralizing antibody, RTCA can be used in a clinical setting to confirm the presence of a bacterial toxin, determine the toxin's concentration, and monitor the efficacy of therapeutic intervention over time. Beyond the clinic, RTCA's sensitivity to dynamic changes in cell health and behavior can be used for diverse research applications, such as identifying a bacterial toxins's binding target on the host cell surface, comparing anti-toxin efficacies, etc.

References – RTCA for Studying Bacterial Toxins (not exhaustive):

1. **Quantitative detection of Vibrio cholera toxin by real-time and dynamic cytotoxicity monitoring.** 2013. J Clin Microbiol. Dec;51(12):3968-74.
2. **Real-time cell-based toxicology testing might replace animal testing for product release and drug safety.** 2008. Biochemica:11-13.
3. **Assessment of Clostridium difficile infections by quantitative detection of tcdB toxin by use of a real-time cell analysis system.** 2010. J Clin Microbiol 48:4129-4134.
4. **Real-time cellular analysis coupled with a specimen enrichment accurately detects and quantifies Clostridium difficile toxins in stool.** 2014. J Clin Microbiol 52:1105-1111.

References – General:

1. **Ultrasensitive Detection and Quantification of Toxins for Optimized Diagnosis of Clostridium difficile Infection.** 2016. J Clin Microbiol 54:259-264.
2. **Diagnosis of Clostridium difficile infection by toxin detection kits: a systematic review.** 2008. Lancet Infect Dis 8:777-784.
3. **Overdiagnosis of Clostridium difficile Infection in the Molecular Test Era.** 2015. JAMA Intern Med 175:1792-1801.

In contrast to the secreted protein toxins described in the previous section, some bacteria effect disease through direct interaction with, or invasion of, host cells. These interactions typically result in changes to the host cell, which can be readily detected via real-time impedance monitoring.

Neisseria meningitidis is the Gram negative bacterium that causes meningitis, a disease which results in developmental impairment or death in about 10% of infected children. Once inside the blood stream, *N. meningitidis* uses type IV pili to bind the apical surface of brain endothelial cells. This interaction induces within the host cell the activation of signaling pathways, gross morphological changes, and the break down of intercellular junctions with neighboring cells. Collectively, these changes are what enable the bacterium to extravasate from brain capillaries and infect the meninges (the protective lining of the central nervous system).[1]

As a tool for studying the key virulence determinants of *N. meningitidis* in real-time, Slanina and coworkers developed an xCELLigence assay in which a confluent monolayer of human brain microvascular endothelial cells (HBMEC) were exposed to isogenic strains of the bacterium.[2] Upon addition of MC58, a clinical isolate of infectious *N. meningitidis*, the impedance signal displays a transient increase followed by a rapid drop to a value of nearly zero **(Figure 8A)**. This drop in the impedance signal correlates with: (1) HBMEC membrane disruption, as evidenced by the release of matrix metalloproteinase 8 (MMP-8) into the medium **(Figure 8B)**, and (2) detachment of the HBMEC from the plate bottom **(Figures 8B-C)**. To assess the importance of the bacterium's capsule in effecting this change, MC58 was compared with an *siaD* isogenic mutant which is deficient for capsule production. In similar fashion, the importance of the *N. meningitidis* lipopolysaccharide (LPS) and OPC membrane protein were also evaluated using isogenic mutants. As seen in **Figures 8D-F**, the bacterial capsule and LPS both have an impact on the kinetics but not the extent of the bacterium's cytopathic effect, whereas OPC is inconsequential in this particular assay.

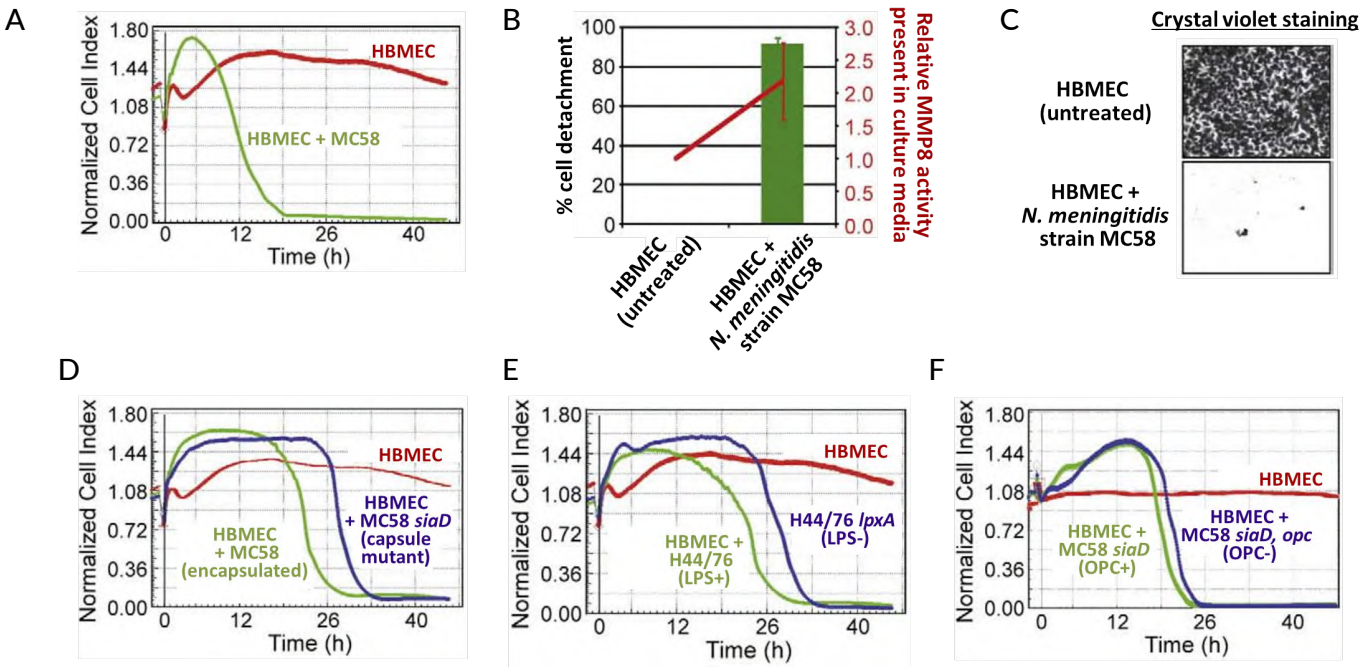

Figure 8. Identifying key virulence factors during *N. meningitidis* infection of HBMEC cells. (A) Infection of HBMEC cells with the MC58 strain of *N. meningitidis* causes a rapid loss in the HBMEC impedance signal, consistent with a cytotoxic effect. **(B)** The drop in impedance signal correlates with target cell detachment and membrane disruption, releasing MMP8 into the culture medium (MMP8 activity was detected via cleavage of a fluorescent substrate). **(C)** Crystal violet staining showing detachment of HBMECs after treatment with MC58. **(D-E)** Comparison of isogenic strains demonstrating that deficiencies in the *N. meningitidis* capsule or LPS slow the cytopathic effect, but do not impact the overall extent of HBMEC killing/lysis. **(F)** Loss of the membrane protein OPC has minimal impact on the cytopathogenicity of *N. meningitidis*. Data adapted from reference 2.

Another noteworthy example of using xCELLigence RTCA to study bacteria-host interactions involves *Salmonella typhimurium*, the causative agent of typhoid. Upon binding to a human intestinal epithelial cell, *S. typhimurium* injects the host cell with bacterial proteins that cause cytoskeletal rearrangements. This process culminates in the host cell's membrane ruffling/protruding outward, and the engulfment of the bacterium within an endocytic vacuole. Inside the vacuole, *S. typhimurium* suppresses normal degradation via fusion with lysosomes and instead turns the vacuole into a bacterial replication compartment.

When Mou and colleagues infected human epithelial HT-29 cells with *S. typhimurium* the host cell-derived impedance signal displayed two distinct peaks, followed by a steady decrease **(Figure 9A)**. Using immunofluorescence microscopy, the first bacterium-induced peak (which is labeled as phase of infection "b" in **Figure 9A**) was found to correlate with membrane ruffling and the deposition of actin stress fibers at the site where the bacterium entered the host cell **(Figure 9B)**. Importantly, when the HT-29 cells were pre-treated with the actin polymerization inhibitor cytochalasin D for 90 minutes prior to infection with S. typhimurium, this first impedance peak was abolished **(Figure 9C)**. Using similar approaches, Mou and coworkers were able to assign distinct molecular/cellular phenomena to different phases of the impedance trace during *S. typhimurium* infection.

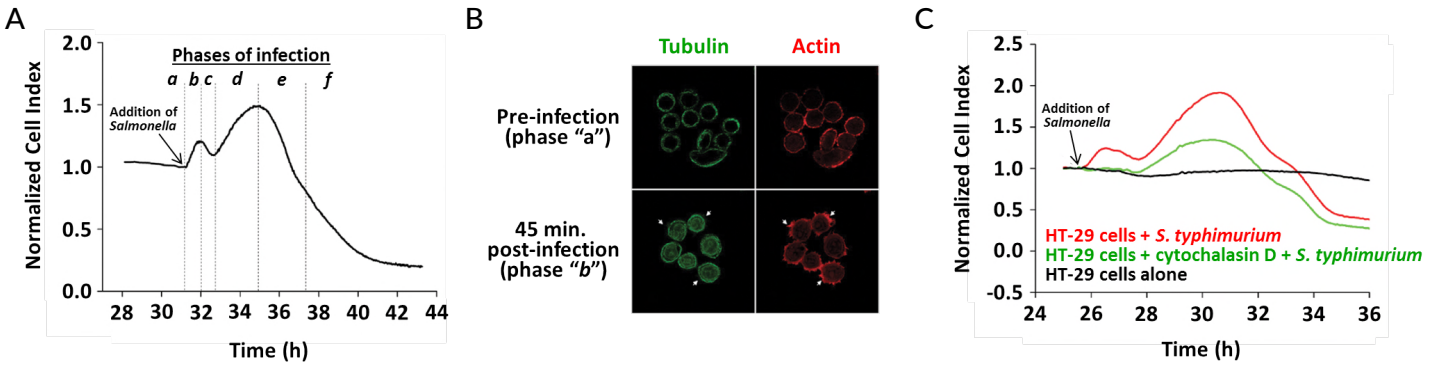

Figure 9. *S. typhimurium* infection of human intestinal HT-29 cells. (A) Immediately after encountering the bacterial cells, HT-29 cells display two spikes in their impedance signal, followed by a steady decrease. Distinct phases of this impedance response have been labeled with letters. **(B)** Immunofluorescent analysis of uninfected and infected HT-29 cells 45 minutes post infection with *S. typhimurium*. Bacterial infection causes tubulin reorganization throughout the host cell, while actin stress fibers accumulate in the immediate vicinity of bacterial entry sites (denoted by white arrows). **(C)** Treating HT-29 cells with the potent actin polymerization inhibitor cytochalasin D for 90 minutes prior to S. typhimurium infection eliminates the first impedance peak, helping to provide a molecular explanation for the cause of this peak. Data adapted from reference 3.

The above study highlights the wealth of information that is contained within real-time impedance traces, and demonstrates the ease with which distinct features of the trace can be correlated with specific molecular or cellular phenomena. xCELLigence RTCA enables these phenomena to be studied in a continuous manner, revealing mechanistic subtleties that would be difficult to piece together using endpoint data alone. This type of information can be used for diverse purposes, such as elucidating which phase of infection a particular gene/protein plays a role in, or screening for drugs that disrupt a distinct step of the infection process.

References – General:

1. **Mechanism of meningeal invasion by Neisseria meningitidis.** Virulence. 2012 Mar-Apr;3(2):164-72.

References – RTCA for Studying Bacteria-Host Interactions (not exhaustive):

1. **Real-time impedance analysis of host cell response to meningococcal infection.** J Microbiol Methods. 2011 Jan;84(1):101-8.
2. **Phenotypic pattern-based assay for dynamically monitoring host cellular responses to Salmonella infections.** PLoS One. 2011;6(11):e26544.
3. **A real-time impedance based method to assess Rhodococcus equi virulence.** PLoS One. 2013;8(3):e60612.
4. **Effect of bacteria used in food industry on the proliferation and cytokine production of epithelial intestinal cellular lines.** J. Functional Foods. 2014; 6: 348-355.

In addition to living in a free-floating "planktonic" state within aqueous environments, bacteria can also colonize biotic and abiotic surfaces at liquid-solid and air-solid interfaces. Within these microenvironments, secreted chemical messengers are used to coordinate gene expression profiles across the colony, thereby promoting survival. A common adaptation of these communities is the secretion of extracellular polymeric substances (EPS), which encapsulate the bacterial cells and protect them from the environment. The ability to form these "biofilms" is a key virulence factor because the EPS matrix facilitates bacterial evasion of host immune responses and also enhances the antibiotic resistance of bacteria as much as 1,000-fold.

Besides playing critical roles in human dental plaque and cavities, chronic infections, rejection of artificial implants, and food poisoning, bacterial biofilms are also responsible for a large percentage of livestock diseases and cause fouling of industrial air and water handling systems, further increasing their economic impact. Though developing drugs to treat biofilms – or prevent their formation in the first place – is of critical importance, the colorimetric assays traditionally used for studying biofilms are inefficient/low throughput, are incompatible with orthogonal assays (i.e. samples are destroyed by the analysis process), and only provide end point data. Multiple research groups have recently described how impedance monitoring by xCELLigence RTCA instruments overcomes each of these limitations, enabling a quantitative and continuous evaluation of biofilms via an assay that is both label-free and totally automated.

As a first step towards understanding what xCELLigence RTCA is capable of monitoring in the context of biofilms, Alex Mira and colleagues demonstrated that both bacterial cells and EPS contribute to the impedance signal (data not shown here). They next assessed the ability of RTCA to screen for biofilm blocking agents (i.e. prophylactic activity) by including antibiotic in the growth media at the time that *S. aureus 240* was seeded into E-Plate wells. Cells were allowed to grow for 20 hours, at which point the Cell Index was compared to an untreated control. In **Figure 10A** the % Cell Index, defined as $[(\text{Cell Index})_{\text{with drug}}/(\text{Cell Index})_{\text{without drug}}]\text{x}100$, is plotted as a function of drug concentration for 10 different drugs. Though each of the 10 antibiotics that were tested displayed prophylactic activity, they did this with differing levels of efficacy. While cefotaxime completely destroyed the biofilm-associated signal at a concentration of 0.25 µg/mL, linezolid required a 128-fold higher concentration to accomplish this **(Figure 10A)**. As a proof of principle, this experiment demonstrates the utility of RTCA as a tool for drug screens aimed at preventing biofilms from forming in the first place.

Of very high clinical relevance is the finding that within particular concentration ranges some antibiotics can actually promote biofilm growth. Being able to characterize this unwanted behavior is critical for preventing physicians from unwittingly exacerbating the very infection they are trying to treat. Importantly, this bifurcated behavior is readily detectable, and quantifiable, using RTCA. While at concentrations of 4-32 µg/mL vancomycin is found to suppress *S. epidermidis* 43040 biofilm growth, at concentrations of 62.5 ng/mL-2 µg/mL biofilm growth is stimulated **(Figure 10B)**.

Next, by allowing a biofilm of *S. epidermidis* 43040 to become established, and subsequently treating it with antibiotics, biofilm disrupting activity was probed. As shown in **Figure 10C**, at concentrations of 0.125 µg/mL-8 µg/mL both cloxicillin and rifampicin were able to induce partial disruption of the biofilm, with the Cell Index dropping by ~60% in the most extreme case. The inability of the ten tested antibiotics to cause complete biofilm disruption is consistent with the known antibiotic resistance of biofilms, demonstrates the importance of testing drug efficacy against the biofilm (rather than planktonic) state, and highlights the need for more effective drugs.

The above experiments demonstrate the utility of xCELLigence RTCA for studying bacterial biofilms. The protocol involves substantially less work than traditional assays: bacteria are simply seeded into an E-Plate, after which data acquisition is continuous and automatic. The real-time nature of the xCELLigence data makes it easy to make quantitative comparisons between different strains and treatments, with both the bacterial cells and their EPS being

evaluable. Achieving such a detailed and nuanced picture of biofilm dynamics using traditional endpoint assays would be prohibitively costly in terms of man hours, and would not provide the same level of reproducibility. The benefits summarized here are described in more detail in a large number of recent publications.

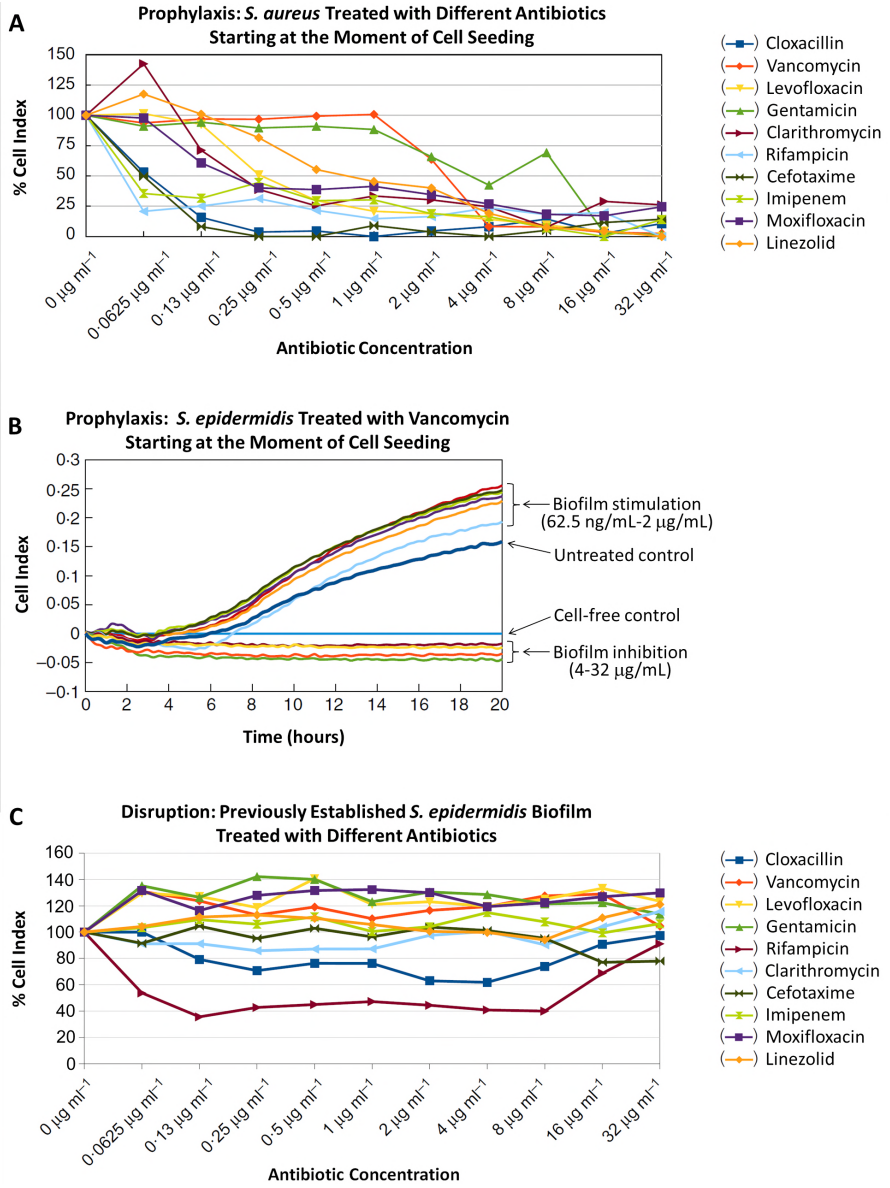

Figure 10. Using RTCA to screen for drugs that either prevent biofilm formation or disrupt established biofilms. **(A)** Ten different antibiotics (each represented by a different colored line) were evaluated for their ability to prevent *S. aureus* 240 from forming biofilm. Antibiotics were present at different concentrations from the moment that bacteria were seeded into wells. 20 hours after seeding, the cell index was measured and compared to the untreated control. The % Cell Index plotted here is simply [(Cell Index)$_{with\ drug}$/(Cell Index)$_{without\ drug}$]x100. **(B)** Testing for prophylactic activity. Depending on its concentration, vancomycin either inhibits or stimulates the growth of *S. epidermidis* 43040 biofilm. **(C)** Testing for biofilm disruption activity. At concentrations above 0.13 µg/mL only cloxacillin and rifampicin are able to induce partial distruption of the *S. epidermidis biofilm*. % Cell Index is defined as described above.

References – RTCA for Studying Biofilms:

1. Use of the Real Time xCelligence System for Purposes of Medical Microbiology. Polish Journal of Microbiol. 2012, 61(3), 191-197.
2. Staphylococcus aureus and MRSA Growth and Biofilm Formation after Treatment with Antibiotics and SeNPs. Int J Mol Sci. 2015 Oct 16;16(10):24656-72.
3. Monitoring in Real Time the Formation and Removal of Biofilms from Clinical Related Pathogens Using an Impedance-Based Technology. PLoS One. 2016 Oct 3;11(10):e0163966.
4. Effect of Antibiotics on Biofilm Inhibition and Induction measured by Real-Time Cell Analysis. J Appl Microbiol. 2016 Dec 8.
5. Bacillus subtilis from Soybean Food Shows Antimicrobial Activity for Multidrug-Resistant Acinetobacter baumannii by Affecting the adeS Gene. J Microbiol Biotechnol. 2016 Dec 28;26(12):2043-2050.
6. Use of Single-Frequency Impedance Spectroscopy to Characterize the Growth Dynamics of Biofilm Formation in Pseudomonas aeruginosa. Sci Rep. 2017 Jul 12;7(1):5223
7. Real-Time Assessment of Staphylococcus aureus Biofilm Disruption by Phage-Derived Proteins. Front Microbiol. 2017 Aug 24;8:1632.

Upon being infected with virus, host cells often display microscopically visible changes that are collectively referred to as a cytopathic effect (CPE). CPEs can include cell shrinkage or enlargement, deterioration, cell fusion, and the formation of inclusion bodies. Not all viruses cause a CPE in their host cell, but when they do, it can be a useful tool for a wide variety of clinical and research applications. In a typical CPE assay a monolayer of cells is inoculated with a virus specimen and then monitored over multiple days (or even weeks) to track morphological changes that emerge in distinct foci corresponding to sites of infection. These types of analyses are laborious and prone to variation due to the subjectivity of identifying and grading CPE foci. As a more efficient, objective, accurate, and higher throughput alternative, a large number of labs have employed xCELLigence RTCA to track viral CPEs for applications such as titer determination, neutralizing antibody analyses, etc. The principle of tracking viral CPEs using impedance is illustrated below in **Figure 11**.

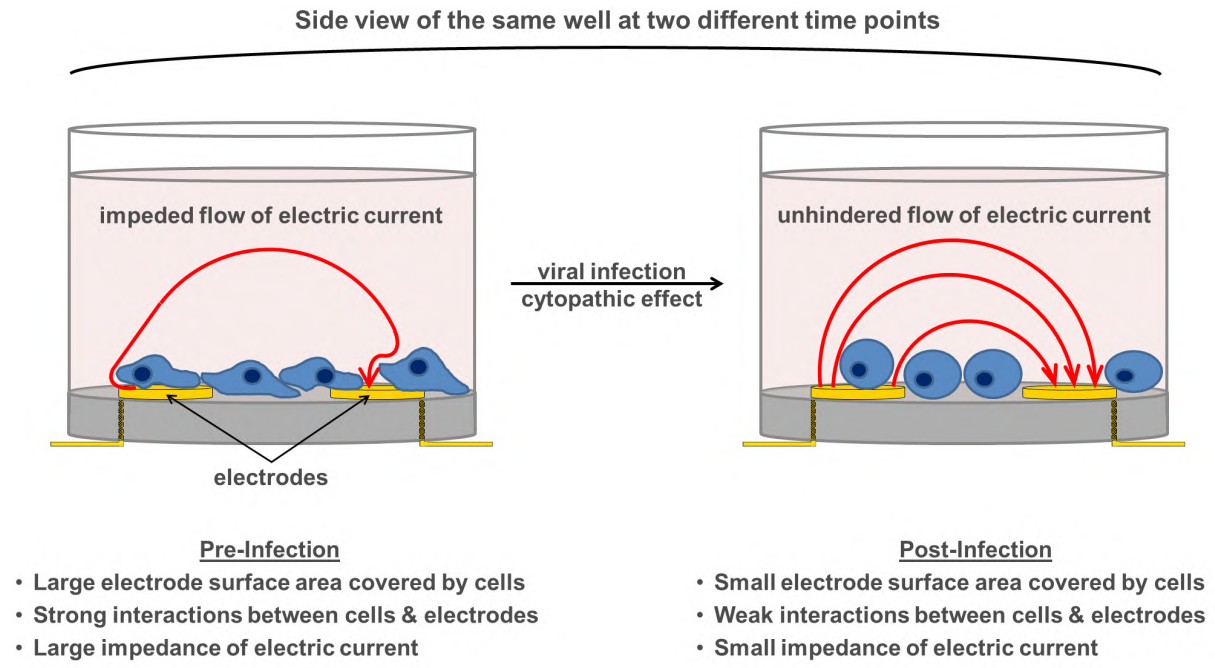

Figure 11. Tracking viral CPEs using xCELLigence RTCA. Within ACEA's E-Plates, virus-induced changes in host cell morphology and attachment strength (hallmarks of a cytopathic effect) are readily detected by changes in the ease with which electric current flows between electrodes. Here, a single well is shown at two different time points (pre- and post-CPE). Note that, for clarity, only two electrodes are shown in the well bottom, and neither the cells nor the electrodes are drawn to scale.

Citing the fact that the traditional CPE/plaque assays used for quantifying viral titers are labor intensive and time consuming, Reisen and colleagues evaluated the efficacy of xCELLigence RTCA for determining the titers of West Nile virus (WNV) and Louis encephalitis virus (SLEV). Vero cells in suspension were incubated with serial dilutions of a known concentration of WMV or SLEV for 30 minutes at 37°C, followed by immediate addition of the cell/virus suspension to E-Plate wells and subsequently monitoring impedance in an xCELLigence instrument. In contrast to uninfected control cells which grew to confluency and maintained a plateaued Cell Index, virus-infected cells displayed a time-dependent decrease in Cell Index down to zero, indicating complete cell lysis **(Figures 12A-B)**. Consistent with the known cytolytic activities of WNV and SLEV, when monitored by xCELLigence WNV displays both an earlier onset of CPE and a more rapid rate of CPE progression.

Importantly, for both WNV and SLEV the time at which the cytopathic effect occurred correlated extremely well with the known titer of the virus. This is highlighted by plotting the CIT50 (time required for the Cell Index to decrease by 50%) as a function of virus titer (lower panels of **Figures 12A-B**). Using this type of standard curve, it is possible to determine the viral titer in samples of unknown concentration. Beyond characterizing viral stocks being used for

research purposes, this approach can be applied in the clinic to quantify the load of a specific virus in patient samples before, during, and after treatment.

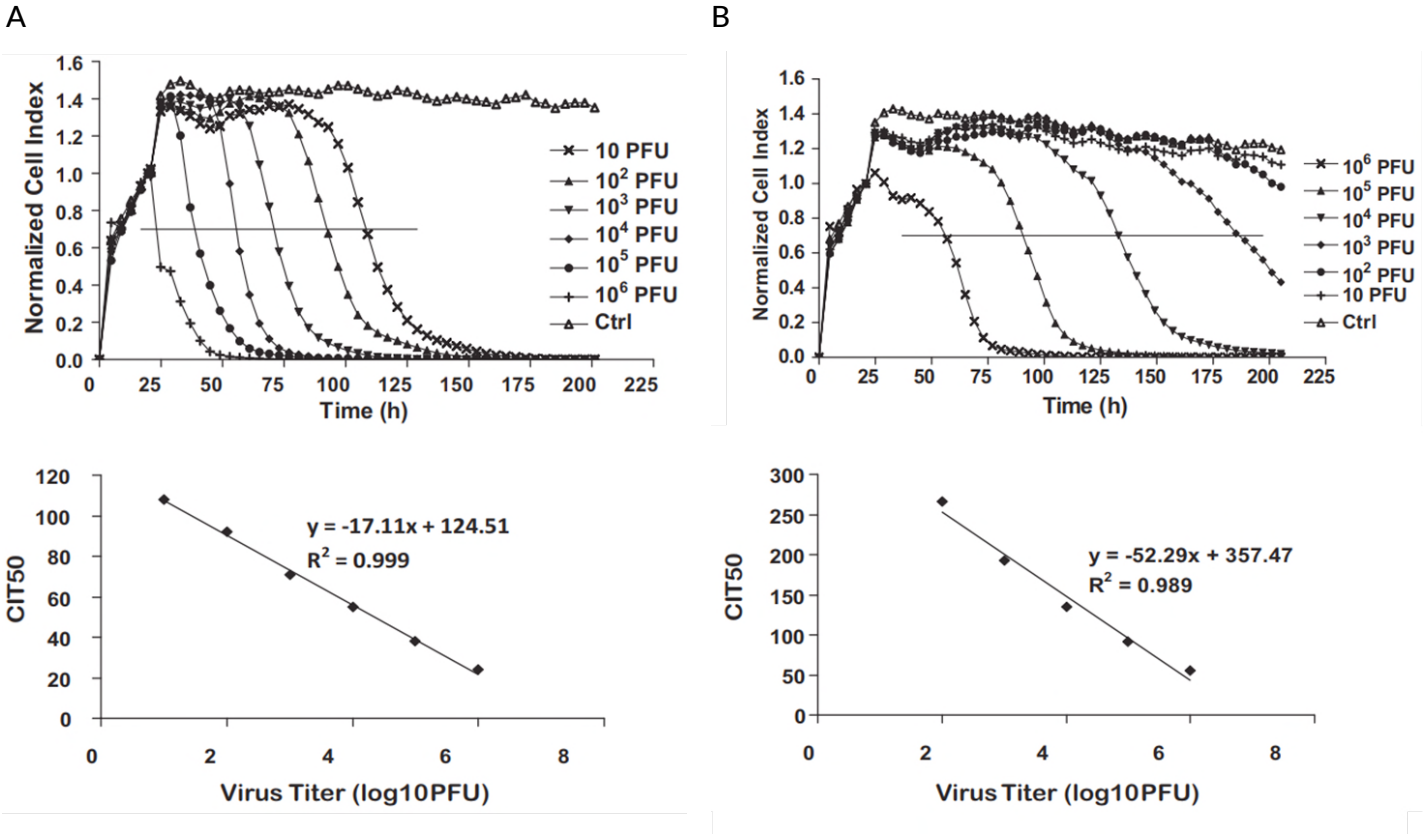

Figure 12. Using xCELLigence RTCA to determine viral titer. (A) Upper panel: Real-time monitoring of WNV-induced cytopathic effect in Vero cells. The normalized Cell Index is shown for E-Plate wells that were inoculated with a negative control (Ctrl) or different numbers of plaque forming units (PFU) of WNV. Each curve is an average of two independent replicate wells. The horizontal line denotes the point at which Cell Index has dropped to 50% of its initial value (i.e. before virus addition). The time required to reach this point is referred to as "CIT50". Lower panel: By plotting CIT50 as a function of viral titer, a standard curve was produced, which can be used for determining virus concentration in clinical samples. **(B)** Real-time monitoring of SLEV-induced cytopathic effect in Vero cells. Experimental details and data processing are similar to part **(A)**. Figure adapted from reference 1.

References – RTCA for Virus Titer Determination:

1. Real-time monitoring of flavivirus induced cytopathogenesis using cell electric impedance technology. J Virol Methods. 2011 May;173(2):251-8.
2. Cellular impedance measurement as a new tool for poxvirus titration, antibody neutralization testing and evaluation of antiviral substances. Biochem Biophys Res Commun. 2010 Oct 8;401(1):37-41.
3. Robust real-time cell analysis method for determining viral infectious titers during development of a viral vaccine production process. J Virol Methods. 2017 Nov 14;252:57-64.

The principles underlying the use of xCELLigence RTCA for monitoring virus-induced cytopathic effects (CPEs) were described in detail on pages 12-13 of this handbook. This real-time viral CPE assay can be employed for diverse applications, including the detection and quantification of neutralizing antibodies, as described below.

After growing Vero cells to confluence in E-Plate wells, Fang and coworkers infected each well with 10^6 plaque forming units of West Nile Virus (WNV) that had been pre-incubated with serially diluted neutralizing antibody of known concentration[1]. As seen in **Figure 13A**, the onset of WNV-induced CPE was delayed by the neutralizing antibody in a manner that was directly dependent on antibody concentration. By plotting the CIT50 (time required for the Cell Index to decrease by 50%) as a function of the antibody titer, a standard curve was generated **(Figure 13B)** which could be used for quantifying the amount of neutralizing antibody present in avian specimens. Importantly, using this standard curve to determine antibody concentrations in infected birds out in the wild gave values that correlated very well with values determined by a traditional plaque reduction neutralization test[1].

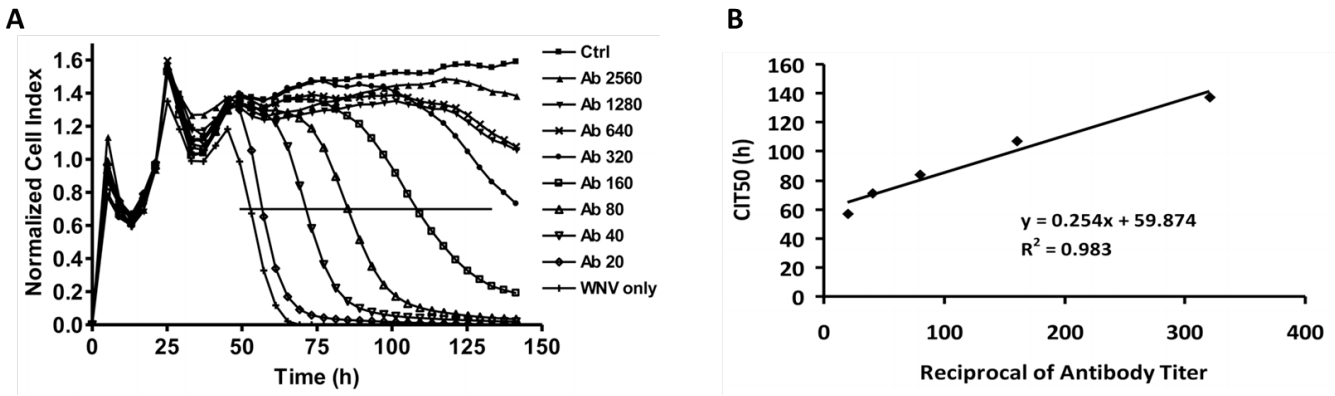

Figure 13. Quantifying WNV neutralizing antibody titer using xCELLigence RTCA. (A) Vero cells were infected with 10^6 plaque forming units of WNV that had been pre-incubated with different dilutions of neutralizing antibody. Ctrl = Vero cells that were not infected with virus; WNV only = Vero cells infected with virus that was not pre-exposed to antibody. The horizontal line denotes the point at which Cell Index has dropped to 50% of its initial value (i.e. before virus addition). The time required to reach this point is referred to as "CIT50". **(B)** By plotting CIT50 as a function of the reciprocal of antibody titer, a standard curve is produced which can be used for assessing the antibody concentrations in wild avian sera. Figure adapted from reference 1.

In a manner similar to that described above for WNV, RTCA has also been used for quantifying the amount of neutralizing antibody against influenza A H1N1 virus that is present in human sera. In short, within E-Plate wells confluent cells were infected with purified H1N1 virus that either had or had not been pre-treated with patient serum **(Figure 14)**. These serum samples had been collected before vaccination, or 7 or 21 days post vaccination, making it possible to track the emergence of an H1N1-specific neutralizing response over time. As expected, the robustness of the H1N1 neutralizing antibody activity increases progressively over the first 21 days post vaccination, evidenced by the delayed onset or complete block of the cytopathic effect.

With its simple, automated workflow and objective and quantitative readout, RTCA clearly offers advantages over traditional assays for detecting and quantifying neutralizing antibodies. This approach provides a simple means for monitoring the efficacy of vaccination, and for elucidating the kinetics of virus resistance emergence.

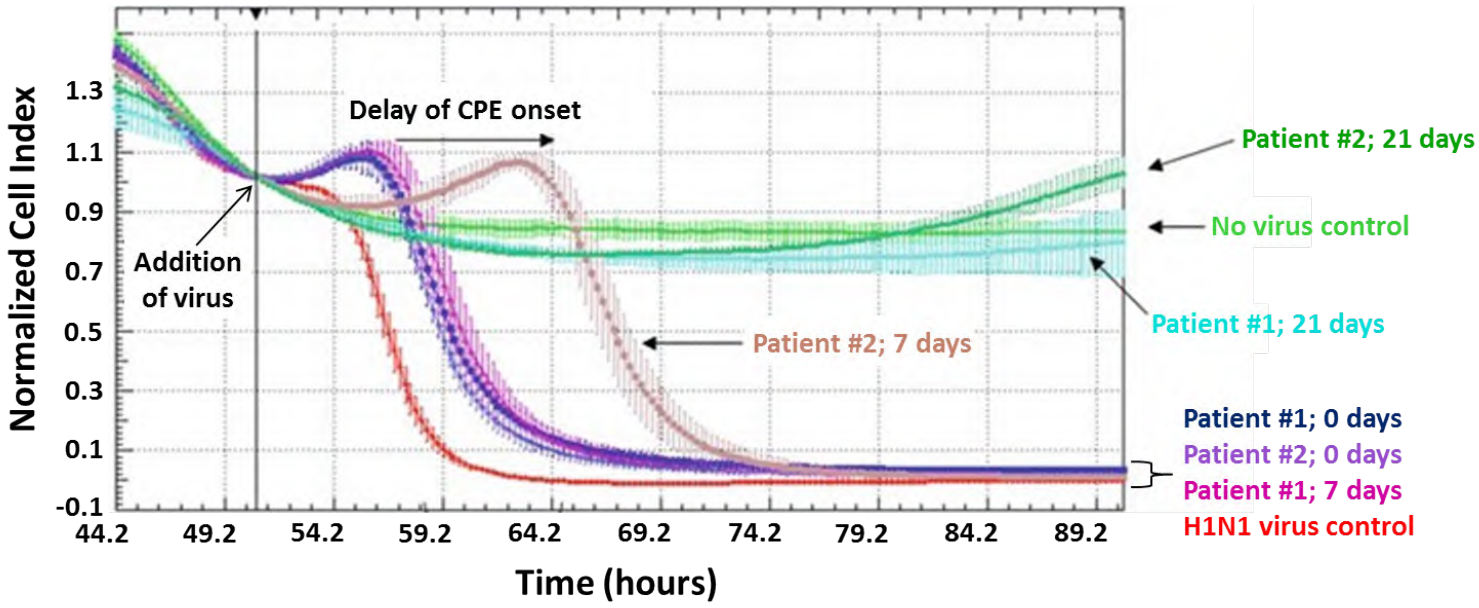

Figure 14. Measuring neutralizing antibody activity in H1N1-vaccinated human subjects by using RTCA to track delayed onset of cytopathic effect. Serum samples from two human patients were collected prior to vaccination (day 0), and then 7 and 21 days post vaccination. These serum samples were incubated with purified H1N1 virus before adding the virus/serum mixture to cells growing in an E-Plate. For both patients, serum from day zero provides no protection and the virus kills the cells with kinetics very similar to the positive control. For patient #2, serum from day 7 showed significant delay of H1N1-induced CPE, indicating the presence of specific neutralizing antibodies against H1N1 virus. In contrast, patient #1's serum at day 7 showed no prophylactic effect, indicating that an H1N1 neutralizing antibody activity was not yet present. However, 21 days post-vaccination the serum from both patients displayed robust neutralizing antibody activity against H1N1, rendering the virus completely incapable of inducing a cytopathic effect. This assay makes it possible to quantitatively assess the efficacy of a particular vaccine, as well as the kinetics of virus resistance emergence. Figure adapted from reference 2.

References – RTCA for Studying Neutralizing Antibodies:

1. Real-time monitoring of flavivirus induced cytopathogenesis using cell electric impedance technology. J Virol Methods. 2011 May;173(2):251-8.
2. Label-free Real-time Cell Based Assay System for Evaluating H1N1 Vaccination Success. Asiabiotech 2010, 14(10): 31-32.
3. Real-time cell analysis--a new method for dynamic, quantitative measurement of infectious viruses and antiserum neutralizing activity. J Virol Methods. 2013 Nov;193(2):364-70.
4. Inhibition of metastasis of rhabdomyosarcoma by a novel neutralizing antibody to CXC chemokine receptor-4. Cancer Sci. 2014 Oct;105(10):1343-50.
5. Novel, real-time cell analysis for measuring viral cytopathogenesis and the efficacy of neutralizing antibodies to the 2009 influenza A (H1N1) virus. PLoS One. 2012;7(2):e31965.

Because real-time impedance monitoring is exquisitely sensitive to virus-induced cytopathic effects, xCELLigence is an excellent tool for identifying and characterizing drugs that inhibit any facet of the virus lifecycle. In one such example, Urs Greber and colleagues at the Institute of Molecular Life Sciences in Zurich aimed to identify a drug that could mitigate the effects of adenovirus in patients already infected with the virus. Their screening assay involved growing HeLa cells to confluence and then infecting them with human adenovirus in the presence of different drug candidates. Most effective among these was flavopiridol, a semisynthetic flavonoid compound known to inhibit the cell cycle dependent kinase Cdk9. As seen in **Figure 15A**, in the absence of drug adenovirus infection induces a robust CPE, with the impedance signal decreasing to zero (red trace). However, in a dose-dependent manner flavopiridol is able to significantly delay the onset of CPE (blue and orange traces). Importantly, these findings based on impedance were corroborated by microscopy analysis **(Figure 15B)**.

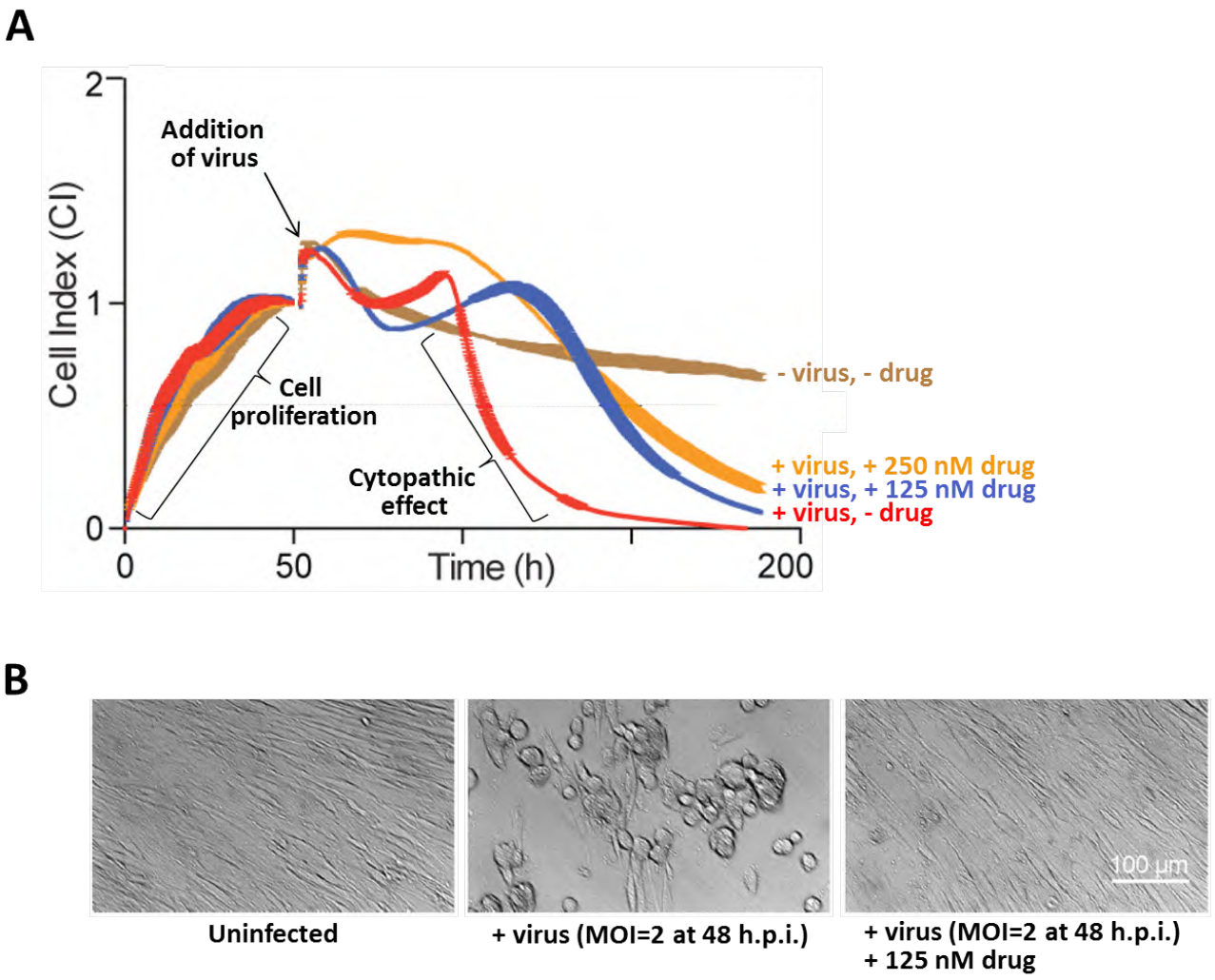

Figure 15. Monitoring antiviral activity of flavopiridol. (A) HeLa cells were grown in an E-Plate to the point of confluence. Roughly 50 hours post seeding, cells were infected with human adenovirus strain C5 in the presence of different concentrations of flavopiridol. **(B)** Flavopiridol affords broad protection against adenovirus. Here WI38 lung fibroblasts were infected with human adenovirus strain D37 and four hours later flavopiridol either was or was not added. 48 hours post infection the drug is clearly seen to have prevented a cytopathic effect from occurring. Data adapted from reference 7.

In a second example, Guy Boivin and coworkers at Laval University in Quebec analyzed the sensitivity of WT and mutant herpes simplex virus 1 (HSV-1) to the antiviral acyclovir. After being grown to confluence in E-Plates, Vero cells were infected with virus for 90 minutes before adding different concentrations of the drug. Although the CPE induced by both WT and mutant virus could be blocked by acyclovir, a much higher concentration of the drug was required for blocking the mutant strain than the WT strain **(Figure 16)**. By plotting the Cell Index value at a given time point as a function of drug concentration, dose response curves were generated (data not shown here), yielding EC50 values of 100 µM and 0.8 µM for the mutant and WT viruses, respectively. Importantly, these findings are consistent with this particular mutant strain of the virus having a mutation in its DNA polymerase, which is the target of acyclovir.

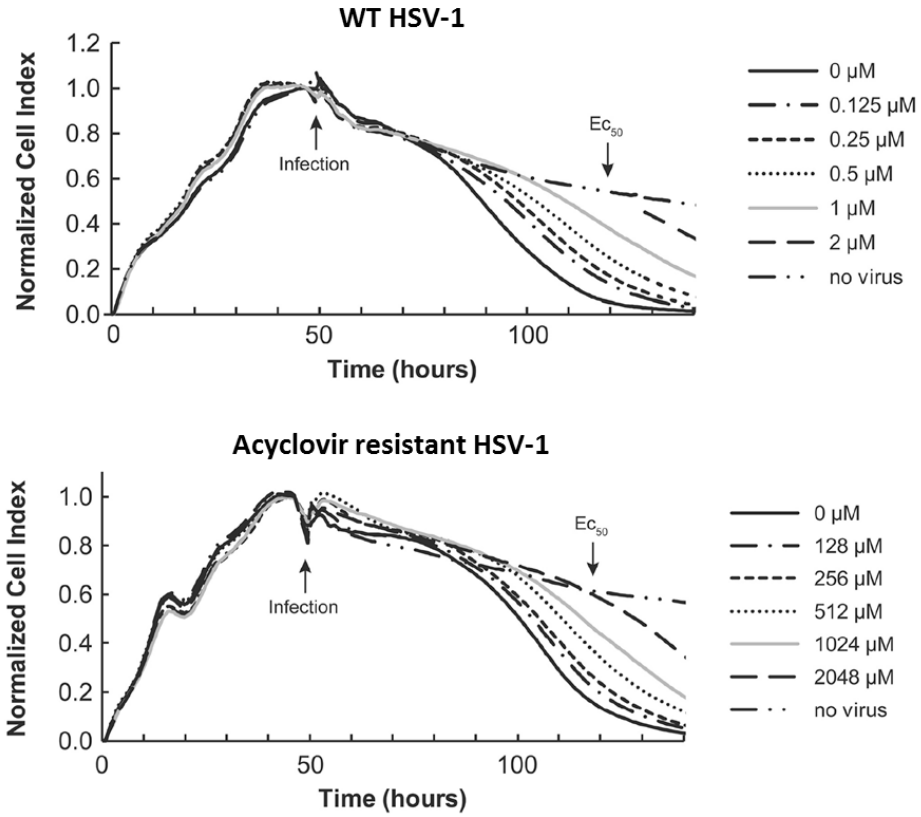

Figure 16. Comparing acyclovir sensitivity of WT and mutant HSV-1. Vero cells were grown to confluence in an E-Plate. 48 hours post seeding cells were infected with either WT or mutant HSV-1 for 90 minutes. Different concentrations of acyclovir were then added and impedance monitored every 30 minutes for an additional 100 hours. Note that much higher concentrations of the drug were required in order to prevent the cytopathic effect for the mutant. Data adapted from reference 5.

References – RTCA for Viral Drug Screening:

1. **A generic screening platform for inhibitors of virus induced cell fusion using cellular electrical impedance.** Sci Rep. 2016 Mar 15;6:22791.
2. **A Real-Time Cell Analyzing Assay for Identification of Novel Antiviral Compounds against Chikungunya Virus.** Methods Mol Biol. 2016;1426:255-62.
3. **Antiviral effects of artesunate on polyomavirus BK replication in primary human kidney cell.** Antimicrob Agents Chemother. 2014;58(1):279-89.
4. **Cellular impedance measurement as a new tool for poxvirus titration, antibody neutralization testing and evaluation of antiviral substances.** Biochem Biophys Res Commun. 2010 Oct 8;401(1):37-41.
5. **Novel Method Based on Real-Time Cell Analysis for Drug Susceptibility Testing of Herpes Simplex Virus and Human Cytomegalovirus.** J Clin Microbiol. 2016 Aug;54(8):2120-7.
6. **Primary cultures of murine neurons for studying herpes simplex virus 1 infection and its inhibition by antivirals.** Acta Virol. 2013;57(3):339-45.
7. **Cell Cycle-Dependent Kinase Cdk9 Is a Postexposure Drug Target against Human Adenoviruses.** ACS Infect Dis. 2017 Jun 9;3(6):398-405.

Living within the intestines or blood vessels of their hosts, parasitic worms (helminths) presently inhabit more than one billion people globally and cause hundreds of thousands of deaths annually. Despite the prevalence and expense of helminth infection, the helminth-specific pharmacopeia is extremely limited. This is historically due, in part, to the paucity of objective high-throughput drug screening methods amenable to the life cycle of these parasites. For many years the primary screening tool has simply been manual monitoring of the rate at which the worms move/writhe when viewed under a microscope.

With the goal of developing a high-throughput anthelmintic drug screening methodology, Smout and colleagues demonstrated that real-time impedance monitoring with xCELLigence RTCA is able to quantify parasitic worm motility (which is a surrogate of viability)[1]. When a parasitic worm is placed within an E-Plate well, its movement changes the electrode surface area being contacted **(Figures 17A-C)**, and consequently the impedance signal fluctuates **(Figure 17D)**. Whereas rapid temporal fluctuation of Cell Index over a broad range of magnitudes is indicative of a fully active worm, slower temporal fluctuation over a narrow range of Cell Index values is indicative of a lethargic/sick/dying worm **(Figure 17D)**. Note that in these types of plots, in order to make the data easier to read, the impedance trace for each condition has been spread out on the Y axis to prevent them from overlapping; the absolute value of the Cell Index isn't important; what is being compared amongst the different conditions is the rate and magnitude of Cell Index fluctuation **(Figure 17D)**.

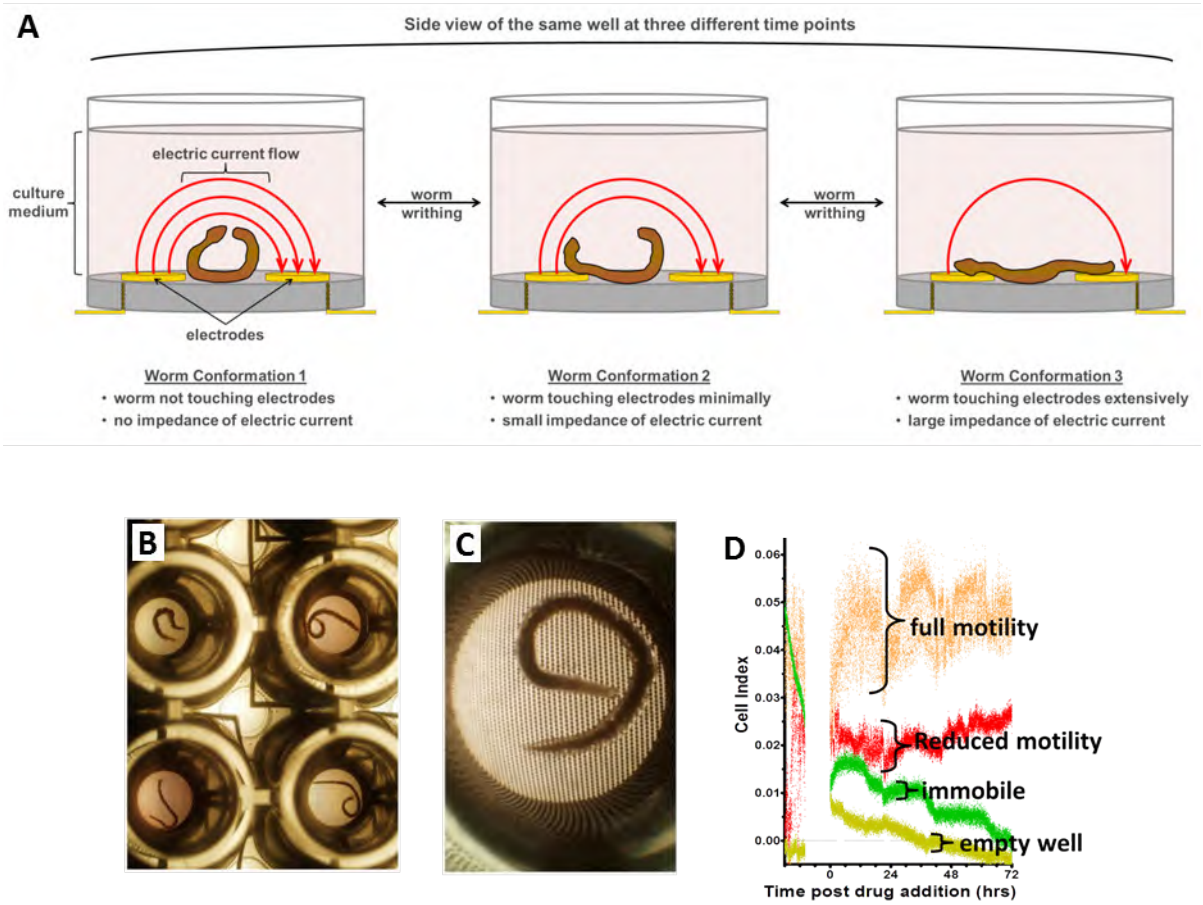

Figure 17. Using RTCA to screen for anthelmintic drugs. (A) As a worm writhes within an E-Plate well, the total electrode surface area that the worm is in contact with changes constantly, thereby causing the impedance signal to fluctuate. **(B)** Micrograph of adult *Ancylostoma caninum* hookworms inside E-Plate wells; while females are shown in the top two wells, males are shown in the bottom two wells. **(C)** Zoomed in view of adult female *Ancylostoma caninum* laying on top of the electrode grid in a well. **(D)** Example data showing distinct impedance traces for healthy vs. drug-impaired worms. Note: the numerical value of the Cell Index is not relevant to this analysis; the curves have been manually repositioned along the Y axis to assist with visualization of the data (i.e. to prevent the four curves from overlapping with one another). The rate at which Cell Index fluctuates, and the magnitude of its fluctuation are the critical parameters here. See text for details. Figures adapted from reference 1, and Michael Smout's unpublished data.

Importantly, using impedance monitoring, Smout and coworkers were able to screen for drug efficacy against three different stages of the parasitic worm life cycle. This is highlighted in **Figures 18A-B**, where levamisole and thiabendazole are shown to effect the L3 larval stage and the egg hatching stage of *Haemonchus contortus*, respectively. In a standard worm motility assay, L3 larvae were lethargic at a levamisole concentration of 0.4 µg/mL, but were killed when the concentration was raised to 6 µg/mL **(Figure 18A)**. To evaluate the effect of thiabendazole on egg hatching, eggs were placed on top of a mesh screen positioned above E-Plate electrodes. As eggs hatched and the larvae crawled through the screen they came into contact with the E-Plate electrodes and caused the impedance signal to increase in a manner that was proportional to the total number of hatched eggs. Thiabendazole was found to suppress this egg hatching process in a dose dependent manner **(Figure 18B)**. These findings are particularly important as they demonstrate that RTCA can be used to cast a very broad net during anthelmintic drug screening: as each stage in a parasitic worm's life cycle may display differential drugability, being able to monitor three of them increases the chances of success.

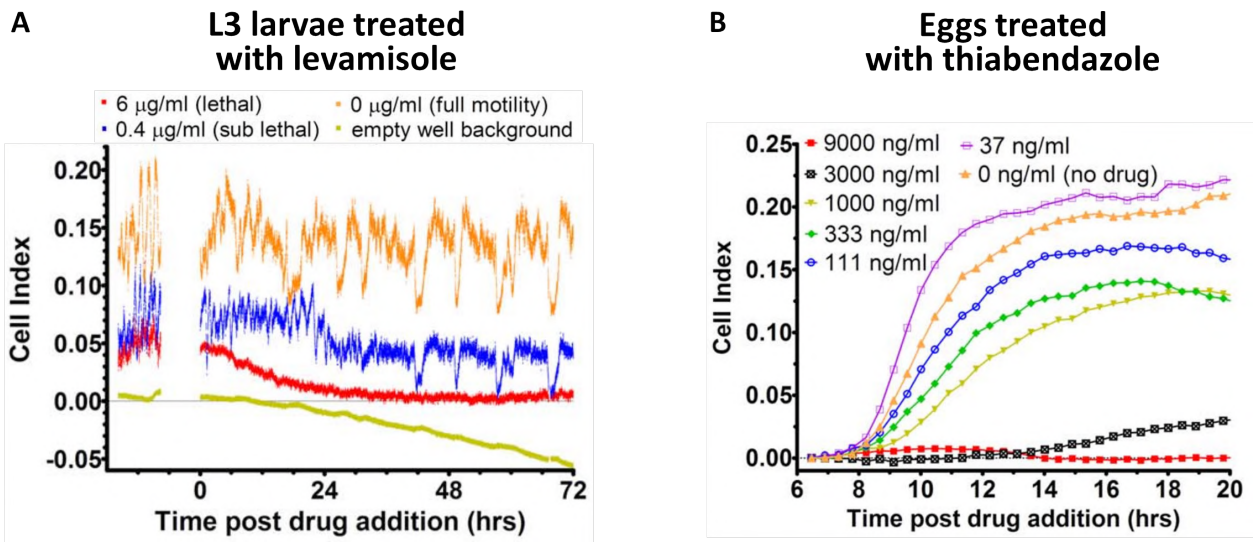

Figure 18. Identifying drugs that are effective against different stages of the *H. contortus* life cycle. (A) Levasmisole is effective against the L3 larval stage. Whereas a concentration of 0.4 µg/mL slightly reduced larval motility, a concentration of 6 µg/mL was lethal. *Note: the numerical value of the Cell Index is not relevant to this analysis; the curves have been manually repositioned along the Y axis to assist with visualization of the data (i.e. to prevent the four curves from overlapping with one another). The rate at which Cell Index fluctuates, and the magnitude of its fluctuation are the critical parameters here. **(B)** Egg hatching in the presence of varying amounts of the drug thiabendazole. Note that increasing drug concentrations result in less egg hatching and therefore a smaller impedance signal. See text for details. Figure adapted from reference 1.

References – RTCA for Studying Parasitic Worms:

1. **A novel high throughput assay for anthelmintic drug screening and resistance diagnosis by real-time monitoring of parasite motility.** PLoS Negl Trop Dis. 2010 Nov 16;4(11):e885.
2. **Viability of developmental stages of Schistosoma mansoni quantified with xCELLigence worm real-time motility assay (xWORM).** Int J Parasitol Drugs Drug Resist. 2015 Aug 6;5(3):141-8.
3. **Reversible paralysis of Schistosoma mansoni by forchlorfenuron, a phenylurea cytokinin that affects septins.** Int J Parasitol. 2014 Jul;44(8):523-31.
4. **Transcriptional Responses of In Vivo Praziquantel Exposure in Schistosomes Identifies a Functional Role for Calcium Signaling Pathway Member CamKII.** PLoS Pathog. 2013 Mar;9(3):e1003254.
5. **Exploration of novel in vitro assays to study drugs against Trichuris spp.** J Microbiol Methods. 2011 Nov;87(2):169-75.
6. **Comparison of novel and existing tools for studying drug sensitivity against the hookworm Ancylostoma ceylanicum *in vitro*.** Parasitology 2012 Mar;139(3):348-57.

Published by:
ACEA Biosciences, Inc.
6779 Mesa Ridge Road Ste. 100
San Diego, CA 92121
U.S.A.

www.aceabio.com

OLS OMNI Life Science GmbH
Germany, Austria +49 421 2761690
info@ols-bio.de | www.ols-bio.de
Switzerland freecall 0800 666 454
info@ols-bio.ch | www.ols-bio.ch

00000 - 20180126 v.3.1